HHS Public Access

Author manuscript

Oncogene. Author manuscript; available in PMC 2016 March 10.

Published in final edited form as:

Oncogene. 2015 September 10; 34(37): 4821–4833. doi:10.1038/onc.2014.410.

Osteopontin Mediates an MZF1-TGF-β1-Dependent Transformation of Mesenchymal Stem Cells into Cancer Associated Fibroblasts in Breast Cancer

Cynthia E. Weber, M.D.[1,3], **Anai N. Kothari, M.D.**[1,3], **Philip Y. Wai, M.D.**[1,3], **Neill Y. Li, B.A.**[1,3], **Joseph Driver, B.A.**[1,3], **Matthew A.C. Zapf, B.A.**[1,3], **Carrie A. Franzen, Ph.D.**[2,3], **Gopal N. Gupta, M.D.**[1,2,3], **Clodio Osipo, Ph.D.**[3], **Andrei Zlobin, Ph.D.**[3], **Wing Kin Syn, M.B.B.S.**[1,4,5], **Jiwang Zhang, Ph.D.**[3], **Paul C. Kuo, M.D.**[1,3], and **Zhiyong Mi, Ph.D.**[1,3]

[1]Department of Surgery Loyola University Medical Center, Cardinal Bernardin Cancer Center, Loyola University Chicago, Maywood, IL, USA

[2]Department of Urology Loyola University Medical Center, Cardinal Bernardin Cancer Center, Loyola University Chicago, Maywood, IL, USA

[3]The Oncology Institute, Cardinal Bernardin Cancer Center, Loyola University Chicago, Maywood, IL, USA

[4]Liver Unit, Barts Health NHS Trust, London, UK

[5]Regeneration and Repair, The Institute of Hepatology, London, UK

Abstract

Interactions between tumor cells and cancer-associated fibroblasts (CAFs) in the tumor microenvironment (TMEN) significantly influence cancer growth and metastasis. Transforming growth factor-β (TGF-β) is known to be a critical mediator of the CAF phenotype, and osteopontin (OPN) expression in tumors is associated with more aggressive phenotypes and poor patient outcomes. The potential link between these two pathways has not been previously addressed. Utilizing in vitro studies using human mesenchymal stem cells (MSCs) and MDA-MB231 (OPN +) and MCF7 (OPN−) human breast cancer cell lines, we demonstrate that OPN induces integrin-dependent MSC expression of TGF-β1 to mediate adoption of the CAF phenotype. This OPN-TGF-β1 pathway requires the transcription factor, myeloid zinc finger 1 (MZF1). In vivo studies with xenotransplant models in NOD-scid mice showed that OPN expression increases cancer growth and metastasis by mediating MSC-to-CAF transformation in a process that is MZF1- and TGF-β1-dependent. We conclude that tumor-derived OPN engenders MSC-to-CAF transformation in the microenvironment to promote tumor growth and metastasis via the OPN-MZF1-TGF-β1 pathway.

Address all correspondence to: Paul C. Kuo, M.D., Loyola University Medical Center, EMS Bldg, Rm 3244, 2160 S. First Ave., Maywood, IL 60153, Phone: 708-327-2710, Fax: 708-327-2852, pkuo@lumc.edu.

Conflicts of interest: The authors have no conflicts of interest to disclose.

Keywords

Osteopontin; Cancer-associated fibroblasts; MZF1; TGF-β1

Introduction

Tumor growth and metastasis is highly dependent on complex dynamic interactions between cancer cells and tumor stroma, mediated by direct cell-cell contact and secreted growth factors and cytokines. CAFs, a tumor stromal element, are involved in tumor growth potentiation, extracellular matrix degradation, tumor cell motility, inhibition of host anti-tumor response, promotion of angiogenesis and metastasis. CAF origin is likely multifactorial, derived from local fibroblasts, bone marrow-MSCs, pericytes and tumor cells. Defining molecular markers and the signal pathways that mediate CAF activation are poorly understood. Nevertheless, it is generally accepted that α-smooth muscle actin (SMA), tenascin-C, vimentin and fibroblast specific protein-1 (FSP-1), among others, describe the CAF phenotype.[1, 2] In addition, TGF-β is critical for CAF activation and elaboration of a pro-tumorigenic microenvironment.[3-6] Signaling by TGF-β regulates tumor initiation, progression and metastasis through tumor cell-autonomous and host–tumor interactions.

OPN, a phosphoprotein secreted by malignant cells and tumor stromal cells, is a key mediator of tumor cell migration and metastasis and a marker of breast cancer progression and metastasis.[7-13] Recent findings suggest that tumor-derived OPN instigates bone marrow-derived MSC trafficking to the TMEN,[14-16] which is characterized by the outgrowth of a desmoplastic stroma rich in CAFs that promotes cancer growth and metastasis.[14, 15, 17] However, a direct relationship between OPN and the CAF phenotype has never been described.

In this study, with in vitro and in vivo human breast cancer models, we demonstrate that OPN induces MSC-to-CAF transformation. OPN binds to cell-surface integrin receptors to activate the transcription factor, myeloid zinc finger 1 (MZF1), and induce MSC production of TGF-β1. The adoption of the CAF phenotype is associated with increased local tumor growth and metastases. Aptamer blockade of OPN abolishes this MZF1-TGF-β1 mediated MSC-to-CAF transformation. This pathway has not been previously characterized.

Results

OPN elicits dose- and time-dependent TGF-β expression in MSCs

MSCs were exposed to OPN at increasing concentrations (0 to 320 ng/ml), and active TGF-β protein expression was measured at 48 h (Figure 1A). The mean concentration of TGF-β1 after exposure to 80 ng/ml was 227±7 pg/ml; 619±14 pg/ml after 160 ng/ml; and 872±4 pg/ml after 320 ng/ml (ANOVA p=0.0001). For TGF-β2 and TGF-β3, after exposure to 80 ng/ml, 160 ng/ml, and 320 ng/ml, mean concentrations of each were ~155 pg/ml, 260 pg/ml, and 425 pg/ml, respectively (ANOVA p=0.0001). Based on this data, in conjunction with the reported median plasma OPN level of 177 ng/ml in metastatic breast cancer patients,[9] all subsequent studies used an OPN dose of 180 ng/ml.[9] MSCs were exposed to OPN at

increasing time intervals (0 to 96 h) (Figure 1B). Time-dependent expression of TGF-β was observed. All isoforms peaked at 12 h. At all time intervals, except TGF-β3 at 96 hours, the increase was significant from baseline ($p<0.05$). Further studies used the 48 h time point.

OPN-mediated TGF-β expression requires integrin cell-surface receptors

OPN binds to αvβ3 integrin and CD44 receptors to mediate important cell-cell and cell-matrix signaling pathways.[18] To examine the role of these cell-surface receptor pathways in OPN-mediated TGF-β expression, MSCs were exposed to OPN and the following inhibitors: RGD, an integrin competitive ligand inhibitor, αvβ3 integrin Ab, CD44 Ab, or APT; control inhibitors: RGE, IgG, and MuAPT (Figure 1C). Extracellular binding of OPN by APT and blockade of integrin and CD44 receptors ablated OPN-mediated active TGF-β1, 2, and 3 expression ($p<0.01$ vs. OPN). The control inhibitors did not alter TGF-β expression. Pharmacologic inhibition of canonical integrin signaling pathways, Src(PP2;10 μM) or FAK(PF228;10μM), abolished OPN-mediated TGF-β expression (Data not shown). These results indicate that OPN-mediated TGF-β expression in MSCs requires OPN binding to integrin receptors, and to a lesser extent, CD44 receptors.

As TGF-β1 expression is up-regulated to a larger degree than other isoforms, remaining studies focus on TGF-β1. A similar expression pattern was seen in total TGF-β1 after OPN exposure (Figure 1D). APT blockade of OPN and integrin receptor blockade resulted in a significant decrease in total TGF-β1 expression ($p<0.01$). However, CD44 receptor blockade had no effect. These results indicate that the primary receptor involved in OPN-mediated TGF-β1 expression in MSCs is likely integrin.

MSC CAF marker expression is OPN-mediated

Expression of OPN-mediated CAF marker (SMA, tenascin-C, vimentin and FSP-1) mRNA was significantly ablated by APT and RGD ($p<0.01$ vs. OPN, OPN+MuAPT and OPN +RGE) (Figure 2A). Of note, on light microscopy, after OPN treatment, MSCs become more elongated and spindle-shaped. Functional correlation using composite zymography demonstrated that OPN increased MSC-associated MMP2 and MMP9 activities by 8- and 5-fold, respectively (Figure 2B). APT and RGD blocked these increases. OPN increased MSC adhesion and migration/invasion by 5- and 2-fold, respectively ($p<0.01$ OPN vs. untreated MSCs) (Figure 2C). APT, RGD and αvβ3 integrin Ab decreased adhesion and migration/invasion to baseline. This data indicates that OPN-integrin interactions in MSCs increase CAF marker expression, MMP activity, adhesion and migration/invasion.

MSCs were exposed to OPN once or daily for one week to determine the duration of CAF marker and TGF-β1 expression. At 2 days, all CAF markers and TGF-β1 were elevated by 8- to 12-fold in both groups ($p<0.01$). In the group exposed once, all CAF markers and TGF-β1 were decreased by day 7 ($p<0.05$). In the daily exposure group, by day 5, TGF-β1 was elevated even further ($p<0.05$). By day 7, tenascin-C and TGF-β1 were elevated compared to day 2 ($p<0.05$) (Figure 2D). These results indicate that under continuous OPN stimulation, as would likely occur an OPN-producing tumor TMEN, a robust and durable CAF marker profile persists and TGF-β1 expression is up-regulated to a similar/larger degree.

To determine the functional role of TGF-β1, its' signaling was blocked using a TGF-β1 type I receptor inhibitor (SB4) or TGF-β1 type II receptor shRNA. OPN-stimulated CAF marker expression was ablated ($p<0.01$ vs. OPN) (Figure 2E). In selected instances, exogenous recombinant TGF-β1 (400 pg/ml) was administered.[19] Exogenous TGF-β1 restored CAF marker expression in OPN+APT+TGF-β1 ($p<0.01$ vs. OPN+APT).

BM-MSCs (3000 cells), enriched from normal human bone marrow, were exposed to OPN. Active TGF-β1 protein increased ~7-fold ($p<0.01$), total: active TGF-β1 ratio was ~8-10:1 (Data not shown). OPN significantly increased CAF marker mRNA expression, which was blocked by RGD and APT ($p<0.01$ vs. OPN) (Figure 2F). Human skin, mammary and lung fibroblasts and murine embryonic fibroblasts were exposed to human OPN. Active TGF-β1 protein and CAF marker expression was not altered (Data not shown). In summary, OPN−integrin binding induces TGF-β1 and CAF marker expression in MSCs.

OPN activates TGF-β1 transcription via MZF1

The role of OPN in TGF-β1 transcriptional regulation was determined by measuring recruitment of RNA polymerase II to a consensus TATA box (ATTA located at −1195bp)[20] and the final exon. TGF-β1 transcription increased ~20-fold after OPN exposure ($p< 0.01$) (Figure 3A). A full-length human TGF-β1 promoter (−3360/+124) was amplified (Figure 3B).[21] Stimulation with OPN resulted in >35-fold transactivation with lesser activation of the first two deletion constructs (Figure 3C). The remaining three deletion constructs showed no activation after OPN stimulation. The 67bp region (−691 to −624) contained a canonical binding site for MZF1 (GGGGAGGAGGGGGA), as predicted by TFSearch.[22, 23] Two MZF1 consensus DNA-binding sequences have been identified: 5′-AGTGGGGA-3′ and 5′-CGGGGAGGGGGAA-3′ (Figure 3D). This G-rich region is 100% homologous to the mouse TGF-β1 promoter (−653 to −637). Human and mouse MZF1 proteins are 83% homologous. MZF1 is involved in cell differentiation, migration and proliferation.[24-27]

ChIP assays targeting −697bp to −600bp confirmed binding of MZF1 and RNA polymerase II to the TGF-β1 promoter in the presence of OPN (Figure 3E). After OPN exposure, MZF1 binding to the G-rich promoter region increased ~18-fold ($p<0.02$ vs. MSCs). This putative MZF1 binding site was mutated to generate two single mutants and one double mutant (Figure 3D). All mutation constructs demonstrated a significant decrease in luciferase activity ($p<0.03$) (Figure 3F). siRNA-mediated silencing of MZF1 significantly decreased TGF-β1 full-length promoter luciferase activity ($p<0.01$), MZF1 and TGF-β1 mRNA ($p<0.01$) and active TGF-β1 protein expression ($p<0.02$) in OPN stimulated MSCs compared to controls (Figure 3G). Taken together, this data indicates that MZF1 regulates OPN-mediated TGF-β1 transcription and protein expression.

OPN induces TGF-β1-dependent MSC CAF marker expression in breast cancer co-cultures

MSCs were co-cultured in Boyden chambers with MB231(OPN+) or MCF7(OPN−) human breast cancer cells. All ELISA and qRT-PCR data presented below are results of media from MSC well or MSC cell lysates only. OPN+ cells exhibit aggressive in vitro indices of adhesion and migration/invasion. OPN− cells exhibit the opposite.[28, 29] MSCs do not express OPN (Data not shown). After 24 h, in MB231+MSC, active TGF-β1 increased 9-

fold compared to baseline; blockade by αvβ3 Ab, RGD and APT abolished the TGF-β1 response ($p<0.01$). Conversely, in MCF7+MSC, active TGF-β1 expression was minimal. Addition of OPN increased active TGF-β1 ~7-fold; this was blocked by αvβ3 Ab, RGD and APT ($p<0.01$) (Figure 4A and B). In co-culture with MB231, CAF marker and TGF-β1 mRNA expression increased 20- to 30-fold ($p<0.01$); abolished by APT, αvβ3 Ab and RGD ($p<0.01$); indicating a causative role for OPN-integrin binding. As expected, exogenous OPN significantly increased CAF marker and TGF-β1 mRNA expression in an integrin-dependent fashion (Figure 4C and D).

Co-culture studies were repeated with SB4, shTGFβR2 and exogenous TGF-β1 (Figure 4E).[19] CAF markers in MB231+MSC were significantly decreased with APT and reversed with exogenous TGF-β1. Similarly, TGF-β1 receptor blockade ablated CAF marker expression ($p<0.01$). This data indicates that tumor-derived OPN interacts with MSC integrin receptors to induce TGF-β1-dependent CAF marker expression. APT blockade of OPN in MB231 co-culture significantly decreased MZF1 mRNA while ablating MZF1 and RNA polymerase II binding to the TGF-β1 promoter region. Conversely, co-culture with MCF7 did not express MZF1 mRNA without exogenous OPN (Figure 4F and G). In parallel with our previous results, this data suggests that OPN mediates MZF1-dependent TGF-β1 expression to induce CAF marker expression in MSCs.

MZF1 and TGF-β1 expression in mouse models

In a MB231+MSC orthotopic xenotransplant model, we previously demonstrated that extracellular OPN blockade and inactivation by APT significantly inhibits: 1) local breast cancer growth and metastasis and 2) MSC expression of CAF markers.[17] This mouse model was repeated to study TGF-β1 and MZF1 expression. Animals were injected via tail vein with APT or MuAPT every 2 days and imaged for 8 weeks. Bioluminescence was greater by 10-fold in MB231+MSC compared with MB231 ($p< 0.01$) (Figure 5A). Local tumor growth showed the same pattern as our original study (Data not shown).[17] At 8 weeks, MSCs were isolated from primary tumors and metastatic sites. In MB231+MSC, MZF1 and TGF-β1 mRNA increased by 4- and 8-fold, respectively, in all locations ($p<0.01$); expression ablated by APT (Figure 5B and 5C). As expected, CAF markers were readily expressed but ablated in the presence of APT (Data not shown).

We have previously reported OPN-mediated EMT (epithelial-mesenchymal transition) associated growth of hepatocellular cancer (HCC) in a mouse xenograft model. [30] To ascertain the role of our newly proposed OPN-MZF1-TGF-β1 axis in HCC, qRT-PCR was performed using cDNA from MSCs isolated by FACS from the primary liver tumors of SK-Hep1+MSC xenografts. APT blockade significantly decreased OPN, MZF1, TGF-β1 and SMA mRNA expression ($p<0.01$), supporting the likely presence of the OPN-MZF1-TGF-β1 axis in HCC (Figure 5D).

A series of xenotransplant experiments was performed using dual-labeled MCF7 cells that constitutively express OPN (RFP-luc-MCF7-lvOPN) implanted alone or co-implanted with GFP-MSCs. A subset of GFP-MSCs had constitutive MZF1 knockdown (MSC(dMZF1)). When MCF7-lvOPN were implanted alone, increased growth did not occur until 8 weeks. In MCF7-lvOPN+MSC mice, tumor growth was significantly greater. Deletion of MZF1

resulted in abrogation of OPN-associated tumor growth in MCF7-lvOPN. In a similar fashion, APT treatment resulted in ablation of tumor growth in MCF7-lvOPN+MSC mice (Figure 6A). After 8 weeks, FACS was used to isolate GFP-MSCs and RFP-MCF7 cells from primary tumors and liver metastases. MCF7-lvOPN+MSC and MCF7-lvOPN+MSC +MuAPT combinations demonstrated significantly greater fractions of tumor cells (RFP+) and MSCs (GFP+), suggesting enhanced local growth and metastasis. Similarly, only MCF7-lvOPN+MSC and MCF7-lvOPN+MSC+MuAPT expressed CAF marker, MZF1 and TGF-β1 mRNA. When compared to MSCs isolated from MCF7-lvOPN+MSC±MuAPT, the MSC(d ZF1)s expressed minimal CAF marker, MZF1 and TGF-β1 mRNA ($p<0.01$) (Figure 6B and 6C). This data demonstrates that enhanced OPN expression in MCF7 in the presence of MSCs promotes local tumor growth and metastasis, which is inhibited by MZF1 ablation in MSCs or APT-inactivation of OPN.

To elucidate the role of TGF-β1, exogenous TGF-β1 (1.2 ng/mouse/day via tail vein) was administered to a subgroup of MCF7-lvOPN+MSC(dMZF1).[31] With this gain-of-function study bypassing the inhibition of MSC elaboration of TGF-β1 in MSC(dMZF1)s, exogenous systemic TGF-β1 accelerated growth and metastasis (Figure 7A and 7B). At Week 5, luciferase activity was enhanced ~10-fold with TGF-β1 ($p<0.01$). Primary tumor MSC(dMZF1)s were isolated by FACS after 6 weeks. CAF markers were strongly expressed with exogenous TGF-β1; MZF1 was not expressed; TGF-β1 was expressed in a positive feedback manner (Figure 7C and 7D).[19] These results indicate that OPN mediates MZF1-dependent TGF-β1 expression in MSCs to promote local tumor growth and metastases via MSC-to-CAF transformation.

Immunohistochemistry of human breast cancer

Immunohistochemical (IHC) staining of normal breast (n=2), ER+PR+ breast cancer (n=2), and triple-negative breast cancer (TNBC) (n=4) tissue samples, obtained under IRB approval by a collaborative researcher, was performed to assess the correlation of OPN, TGF-β1, MZF1 and SMA expression. When comparing normal and ER+PR+ (luminal) breast tissue to TNBC, basal-like thus histologically similar to MB231, there is a definite difference in quantity and intensity of staining of these proteins (Figure 8). In addition to the expected higher-grade phenotypic features (minimal tubule formation and enlarged nuclear size and pleomorphism), the aggressive, poorer prognosis TNBC displays increased cytosolic expression of all four proteins in the tumor cells and stromal elements. In TNBC, the quantity of nuclear staining of MZF1 is also increased. The data obtained from this limited IHC analysis is not enough to draw any conclusion regarding prognostic value of the OPN-MZF1-TGFβ1 axis, but it does pave the way for future studies to examine this more closely. This would add to the current data supporting OPN as a prognostic marker for breast cancer. [32, 33]

Discussion

The TMEN significantly influences tumor behavior.[6, 34-37] CAFs are a critical constituent, residing within the tumor or its margins. However, there is lack of an accepted biomarker definition and controversy over the cell of origin and location of the CAF precursor

cell.[1, 35, 38, 39] Utilizing in vitro and in vivo models of human breast cancer, we demonstrated that: 1) OPN induces MZF1-dependent TGF-β1 production in MSCs to promote local tumor growth and metastasis, 2) MSCs adopt a CAF phenotype as the result of autocrine TGF-β1 signaling, and 3) inactivation of extracellular OPN by the OPN-R3 aptamer blocks TGF-β1-mediated MSC-to-CAF transformation and tumor growth and metastasis. The OPN-MZF1-TGF-β1 signaling pathway has not been previously described.

CAFs are specialized stromal cells with myofibroblast features that promote in vitro cell proliferation, in vivo tumor growth and facilitate by producing tumor-promoting cytokines such as CCL5, TNF, IL-6 and SDF1.[40, 41] Additionally, CAFs might be a critical niche component, protecting cancer stem cells; a small proportion of cancer cells responsible for cancer metastasis, drug resistance and disease relapse; from the effects of chemotherapy. Small numbers of MSCs, multipotent cells primarily located in bone marrow, can be detected in other tissues where they may serve as sources of dormant stem cells.[42-45] Data from animal and human breast cancer models suggests that a significant proportion of CAFs are derived from circulating BM-derived MSCs.[46, 47] Thus, eliminating CAFs and/or repressing the generation of CAFs from local and BM-derived MSCs might be an effective therapeutic strategy against cancer, especially in combination with standard chemotherapy.

OPN is a ligand for αvβ3 integrin and CD44 receptors.[18, 48, 49] Elevated plasma OPN correlates with increased breast cancer tumor burden, metastasis and prognosis.[11, 50-52] OPN inhibition decreases local breast cancer growth and metastasis.[17, 28, 29, 53-55] Therefore, OPN has been proposed as an anti-cancer target. Studies suggest that OPN-integrin binding via the RGD domain stimulates tumor cell invasiveness and migration, in part through activation of MMPs/uPA. On-going research in our lab has identified the likely involvement of PKA signaling in the OPN-MZF1-TGFβ1 axis. Our current hypothesis is that PKA is activated downstream of integrin which then leads to MZF1 up-regulation. Further experiments are underway to test this hypothesis. OPN binds to CD44 to promote cell survival, chemotaxis, homing and adhesion to enhance metastatic behavior, suggesting a direct effect of OPN on tumor cells.[56-58]

Immunohistochemical studies demonstrate that OPN localizes to the leading edge of invading tumors, which are enriched in MSC-like cells, suggesting that OPN+ cells interact in a paracrine fashion with TMEN constituents.[59-61] In animal models, OPN produced by tumor and stromal cells stimulates the incorporation of activated BM-derived cells into breast tumors, instigating local growth and distant metastases.[14, 62] Large numbers of BM-MSCs were found in explanted tumors and metastases as shown by GFP+ BM transplantation studies. By description, this is similar to our findings.[17] In xenograft studies with 4T1(OPN+) murine breast cancer cells (spontaneous metastatic model),[63] MSCs injected into circulating blood selectively localized and proliferated in subcutaneous and metastatic sites. However, the signaling pathways that underlie OPN-induced MSC accumulation in tumors remain unknown.

TGF-β mediates fibroblast differentiation, tumor stroma formation and regulates all stages of tumor development via tumor cell-autonomous and host-tumor interactions.[3-6] Resident fibroblasts and bone marrow-derived MSCs convert into CAFs during tumor progression, a

TGF-β autocrine/paracrine signaling loop acts to initiate/maintain this CAF phenotype and CAFs increase tumor invasion.[19, 64-66] The loss of TGF-β1 reverses the growth advantage imparted by CAFs.[67] These studies demonstrated the role of TGF-β signaling in CAF initiation and maintenance. However, the initiating steps for TGF-β synthesis have never been addressed. Serendipitously, OPN induces TGF-β expression and fibroblast activation in models of inflammation and fibrosis.[68-75] In the context of carcinogenesis, our findings indicate that tumor-derived OPN stimulates TGF-β1 production and subsequently the CAF phenotype in MSCs.

MZF1, originally isolated from a myelogenous leukemia patient, is a Kruppel family transcription factor containing 13 C2H2 zinc fingers. MZF1 forms a peptide loop that binds to G-rich DNA consensus sequences.[22, 23, 27] Genes regulated by MZF1 identified thus far include: CD34, lactoferrin, myeloperoxidase, PADI1 and N-cadherin.[76] A few reports identify MZF1 as a tumor suppressor, namely an in vitro cervical cancer model [24] and an in vivo knockout model [27]; however the majority of recent literature supports the oncogenic nature of MZF1 we describe.[23, 25, 26, 76, 77] Expression of MZF1 is associated with the anti-apoptotic and oncogenic transformation of cervical (SiHA, HeLa) and colorectal (Rko, SW480) cancer cell lines.[76] 3T3 cells transduced with MZF1 lose contact inhibition and substrate dependence, while undergoing more rapid cell cycling; in athymic mice, these transduced 3T3 cells form aggressive fibrosarcomas.[23] An MZF1 antisense oligonucleotide inhibits PKCα expression and decreases cell migration and invasion in HCC (SK-Hep1).[77] The role of MZF1 in TGF-β1 expression has never been described, but the link to N-cadherin and the overlap between EMT and CAF markers correlates with the role of MZF1 in MSC-to-CAF transformation.

RNA aptamers are short ssRNA oligonucleotides that specifically bind extracellular protein targets such as OPN.[78, 79] Aptamers possess many useful properties as potential therapeutic molecules: they are small (8-15kD) synthetic compounds with high target affinity (K_d~0.05-10nM), are heat stable, site-specific modifications can be made to alter bioavailability and mode of clearance and have minimal interbatch variability. Animal studies have shown that aptamers are well tolerated, exhibit little immunogenicity and are likely suitable for repeated administration.[78, 79] The aptamer pegaptanib was approved for treatment of macular degeneration.[80] Our work indicates that OPN-R3 APT may serve a role in targeting CAF phenotype activation.

In summary, we have characterized a signaling pathway by which OPN interacts with MSCs via integrin receptors to up-regulate MZF1-mediated expression of TGF-β1, which results in conversion of MSCs to a CAF phenotype with promotion of more aggressive local tumor growth and metastasis. Blockade and inactivation of extracellular OPN by the OPN-R3 aptamer effectively abolishes this pathway. This suggests that OPN blockade may be an effective clinical strategy for tumor growth inhibition.

Materials and Methods

Materials

The pharmacologic properties and sequences of OPN-R3 aptamer (APT) and mutant aptamer (MuAPT) have been previously published.[28]

Recombinant human OPN and TGF-β1 proteins (R&D Systems, Minneapolis, MN); αvβ3 integrin and CD44 Abs (Santa Cruz Biotechnology, Santa Cruz, CA); Arg-Gly-Asp (RGD), Arg-Gly-Glu (RGE) (Sigma-Aldrich, St Louis, MO); SB431542 a TGF- β1 type I receptor inhibitor (EMD Millipore, Billerica, MA); TGF-β1 type II receptor shRNA (Santa Cruz Biotechnology); MZF1 siRNA (Life Technologies, Carlsbad, CA); and Control siRNA[81]: UAAGGCUAUGAAGAGAUAC were all obtained.

Cell culture

Human MSCs (CD105+/CD73+/CD44+ and CD34−/CD45−/CD14−/HLA−DR−; Texas A&M Institute for Regenerative Medicine, Bryan, TX) were maintained in MEMα with 20% FBS; a subset was GFP+. Transduction with MZF1 siRNA generated MSCs with constitutive knockdown of MZF1 (MSC(dMZF1)) for use in animal studies. After IRB approval, primary human MSCs (BM-MSCs) were isolated using RosetteSep Human Mesenchymal Stem Cell Enrichment Cocktail (STEMCELL, Vancouver, Canada) from normal human BM isolates. Human MDA-MB231 and MCF7 breast cancer cell lines, purchased from American Type Culture Collection (ATCC, Manassas, VA), were maintained in DMEM with 10% FBS. Lentiviral transduction (GenTarget Inc, San Diego, CA) was used to generate dual-labeled RFP-Luc-MB231 and RFP-Luc-MCF7 cells for use in animal studies. Further manipulation using lentiviral transduction generated MCF7 cells that constitutively express OPN (RFP-Luc-MCF7-lvOPN). Human skin fibroblasts (CCD-1140SK), human lung fibroblasts (MRC-5), and murine embryonic fibroblasts (CF-1) were purchased from ATCC. Human mammary fibroblasts were a gift from Dr. Kuperwasser, Tufts University.

Co-culture

1:1 ratio of cancer cells to MSCs were plated in Boyden Chamber (Corning Inc, Corning, NY) wells with 0.4μm pores that allow cytokine and growth factor passage but prevent cell movement.

Adhesion and invasion assays

Adhesion assays were performed on 96-well plates coated with 10 μg/ml Matrigel. Cells were trypsinized and re-suspended in DMEM with 1% BSA, 1mM MgCl2, 0.5mM CaCl2 at 1×10^6 cells/ml. 1×10^5 cells (100 μl) were added per well and incubated for 30 min at 37°C in 5% CO_2. Non-adherent cells were removed (PBS wash with 1mM MgCl2 and 0.5mM CaCl2). Adherent cells were fixed with 3.7% paraformaldehyde, rinsed with PBS and stained with 0.4% crystal violet. The dye was released by addition of 30% acetic acid and plates were read in a microplate reader (Molecular Devices, Sunnyvale, CA) at 590nm. For invasion assays, cells were seeded at 10^5 cells per well in the upper chamber of 12-well Boyden Chamber transwells (8μm pore). After incubation, cells on the top surface of filters

were removed with cotton swabs. Adherent cells were fixed, dyed and measured as described above.

Quantitative Real-time PCR

qRT-PCR was performed with the two-step reaction protocol using iQ SYBR Green detection kit (Bio-Rad Laboratories, Hercules, CA). First-strand cDNA were synthesized from 1.0 μg of total RNA using the iScript Select cDNA synthesis kit (Bio-Rad Laboratories). Reaction protocol: 25°C for 5 min, 42°C for 30 min, and 85°C for 5 min. The qRT-PCR parameters were: 95°C for 3 min; 95°C for 30 seconds, 55°C for 35 seconds (40 cycles); 95°C for 1 min, and 55°C for 10 min. ΔΔCT was calculated after β-actin normalization.

Primer Sequences

SMA	5′-TAGCACCCAGCACCATGAAGAT-3′
	5′-GAAGCATTTGCGGTGGACAATG-3′
Vimentin	5′-AGAACGTGCAGGAGGCAGAAGAAT-3′
	5′-TTCCATTTCACGCATCTGGCGTTC-3′
Tenascin-C	5′-AGCATCACCCTGGAATGGAGGA-3′
	5′-TGTGGCTTGTTGGCTCTTTGGA-3′
FSP-1	5′-TGTCCTGCATCGCCATGATGTGTA-3′
	5′-TGAACTTGCTCAGCATCAAGCACG-3′
TGF-β1	5′-TGGCGATACCTCAGCAACC-3′
	5′-CTCGTGGATCCACTTCCAG-3′
MZF1	5′-AGTGTAAGCCCTCACCTCC-3′
	5′-GGGTCCTGTTCACTCCTCAG-3′
β-actin	5′-AGAGGGAAATCGTGCGTGAC-3′
	5′-CAATAGTGATGACCTGGCCGT-3′

Enzyme-linked immunosorbent assay (ELISA)

Supernatants were analyzed using TGF-β ELISAs (R&D Systems). Measurement of the active form required no manipulation; total protein measurement required acidification (1N HCl followed by 1.2N NaOH/0.5M HEPES) prior to assay.

Construction of promoter plasmids

Human genomic DNA was isolated from normal human lung fibroblasts (ATCC CCL-210). TGF-β1 promoter region was defined using NCBI Reference Sequence NM_000660.4. Full-length promoter (−3360/+124) and deletion constructs (−1196/+124; −691/+124; −624/+124; −551/+124; −220/+124) were generated by PCR, setting the ATG start site as 0. All promoter fragments were cloned into pGL4.10(luc2) vectors (Promega, Madison, WI) to generate luciferase-reporter constructs.

Construction of promoter mutations

Point mutations of the TGF-β1 promoter MZF1 putative binding site were made using the QuikChange II Site Directed Mutagenesis Kit (Agilent Technologies, Santa Clara, CA). These mutated promoter fragments were cloned into pGL4.10(luc2) vectors and direct sequencing analysis confirmed.

Dual luciferase reporter assay

4 ug of the luciferase-reporter constructs or empty pGL4.10(luc2) vector were co-transfected with 0.4 ug of Renilla into MSCs and treated with OPN. After 48 h, using a Dual-Luciferase assay system (Promega), cells were lysed and promoter activity was measured as a ratio of Firefly:Renilla luciferase using the Modulus Luminometer (Promega).

ChIP RT-PCR

Cells were treated with OPN and cultured for 48 h prior to DNA cross-linking and lysis. Chromatin was fixed and immunoprecipitated using the EZ-ChIP assay kit (EMD Millipore). For the RNA Polymerase II ChIP assay, purified chromatin was immunoprecipitated using 1 ug of RNA Polymerase Ab or normal mouse IgG (negative control). For the MZF1 ChIP assay, chromatin was immunoprecipitated using 1 ug of MZF1 Ab, RNA Polymerase Ab (positive control), or normal rabbit IgG (negative control). DNA was sonicated to 500bp fragments. After DNA purification, RNA polymerase II binding to the TGF-β1 TATA box and final exon and MZF1 binding to the putative site on the TGF-β1 promoter was determined by qRT-CPR. CT values were normalized to β-actin. Products from qRT-PCR were run on agarose gel to visualize bands. ChIP RT-PCR primers:

TATA box:	F 5′-CCCAGCCTGACTCTCCTTCCGTTC-3′
	R 5′-GGTGATCCAGATGCGCTGTGGCTT-3′
Final exon:	F 5′-GGTGGAGCAGCTGTCCAACATGAT-3′
	R 5′-GCACGGGTGTCCTTAAATACAGCC-3′
MZF1:	F 5′-GAGCTCGCCCCAGAGTCTGAG-3′
	R 5′-CGCGCCTCCGGCTCGCAGCGG-3′

Zymography

Gelatin zymography used the Novex Zymogram Gel (Life Technologies) system. Concentrated serum-free MEM collected from MSC cultures was mixed with sample buffer and loaded on 10% gel. After running for 1.5 h, the gel was incubated in renaturing buffer for 30 min at room temperature. After incubating the gel with developing buffer at 37°C overnight, the gel was stained and images were acquired by AlphaImager 3400 (Protein Simple, Santa Clara, CA).

Mouse xenograft model

Loyola University's Animal Care and Use Committee approved animal protocols. Six-week-old female NOD-scid mice (Jackson Laboratory, Bar Harbor, ME) were implanted with 10^6

dual-labeled cancer cells and GFP-MSCs and injected with APT or MuAPT as previously described.[17] After administration of D-luciferin (150 mg/kg), anesthetized mice (intraperitoneal ketamine (75 mg/kg) and xylazine (10 mg/kg)) were imaged with the IVIS 100 Imaging System (PerkinElmer, Waltham, MA). Bioluminescence is reported as the sum of detected photons/second from a constant region of interest. Baseline tumor volume was established at day 2. Prior to necropsy, D-luciferin was injected to perform ex vivo imaging of primary, lung and liver tumors.

Fluorescence activated cell sorting

Single cell suspension was prepared as described.[82] Cells were sorted using BD FACSAriaIII (BD Biosciences, Franklin Lakes, NJ). For GFP, cells were excited using a 488nm laser, with emission collected through a 530/30 bandpass filter. For RFP, cells were excited using a 561nm laser, with emission collected through a 610/20 bandpass filter.

Immunohistochemistry

Human breast cancer tissue samples (IRB approved) formalin fixed, paraffin embedded, sectioned to 5μm, rinsed and followed by antigen unmasking utilizing Leica ER2 (Leica Biosystems, Richmond, IL) concentrated EDTA retrieval solution. Tissues were stained with OPN, TGF-β1, MZF1 and SMA antibodies using modified Protocol F, staining was detected using Leica refine DAB kit, slides were rinsed, counterstained, dehydrated and mounted.

Statistical Analysis

All experiments were done in triplicate. Data are presented as mean±SD. Analysis utilized Student's t-tests and ANOVA. Values of $p<0.05$ were considered significant.

Supplementary Material

Refer to Web version on PubMed Central for supplementary material.

Acknowledgments

The research was supported by NIH grants: GM65113, CA155306 and UL1 RR024128.

The authors would like to thank Andy Hall, Research Histology Manager, at the University of Illinois at Chicago Research Resources Center who performed all immunohistochemical staining and mounting.

The authors would also like to thank Dr. Dariusz Borys, of the Loyola Department of Pathology, for assistance with imaging of slides.

References

1. Mishra PJ, Humeniuk R, Medina DJ, Alexe G, Mesirov JP, Ganesan S, et al. Carcinoma-associated fibroblast-like differentiation of human mesenchymal stem cells. Cancer Res. 2008; 68:4331–4339. [PubMed: 18519693]
2. Spaeth EL, Dembinski JL, Sasser AK, Watson K, Klopp A, Hall B, et al. Mesenchymal stem cell transition to tumor-associated fibroblasts contributes to fibrovascular network expansion and tumor progression. PLoS One. 2009; 4:e4992. [PubMed: 19352430]
3. Bierie B, Moses HL. Tumour microenvironment: TGF[beta]: the molecular Jekyll and Hyde of cancer. Nat Rev Cancer. 2006; 6:506–520. [PubMed: 16794634]

4. Worthington JJ, Klementowicz JE, Travis MA. TGFbeta: a sleeping giant awoken by integrins. Trends Biochem Sci. 2011; 36:47–54. [PubMed: 20870411]
5. Liu Z, Bandyopadhyay A, Nichols RW, Wang L, Hinck AP, Wang S, et al. Blockade of Autocrine TGF-beta Signaling Inhibits Stem Cell Phenotype, Survival, and Metastasis of Murine Breast Cancer Cells. J Stem Cell Res Ther. 2012; 2:1–8. [PubMed: 23482850]
6. Dumont N, Liu B, Defilippis RA, Chang H, Rabban JT, Karnezis AN, et al. Breast Fibroblasts Modulate Early Dissemination, Tumorigenesis, and Metastasis through Alteration of Extracellular Matrix Characteristics. Neoplasia. 2013; 15:249–262. [PubMed: 23479504]
7. Ye QH, Qin LX, Forgues M, He P, Kim JW, Peng AC, et al. Predicting hepatitis B virus-positive metastatic hepatocellular carcinomas using gene expression profiling and supervised machine learning. NatMed. Apr; 2003 9(4):416–23. 2003; 9: 416-423.
8. Wai PY, Kuo PC. Osteopontin: regulation in tumor metastasis. Cancer Metastasis Rev. 2008; 27:103–118. [PubMed: 18049863]
9. Bramwell VH, Doig GS, Tuck AB, Wilson SM, Tonkin KS, Tomiak A, et al. Serial plasma osteopontin levels have prognostic value in metastatic breast cancer. Clin Cancer Res. 2006; 12:3337–3343. [PubMed: 16740755]
10. Mi Z, Guo H, Wai PY, Gao C, Wei J, Kuo PC. Differential osteopontin expression in phenotypically distinct subclones of murine breast cancer cells mediates metastatic behavior. JBiolChem. Nov 5; 2004 279(45):46659–67. Epub2004Aug30 2004; 279: 46659-46667.
11. Singhal H, Bautista DS, Tonkin KS, O'Malley FP, Tuck AB, Chambers AF, et al. Elevated plasma osteopontin in metastatic breast cancer associated with increased tumor burden and decreased survival. ClinCancer Res. 1997; 3:605–611.
12. Cook AC, Tuck AB, McCarthy S, Turner JG, Irby RB, Bloom GC, et al. Osteopontin induces multiple changes in gene expression that reflect the six "hallmarks of cancer" in a model of breast cancer progression. Mol Carcinog. 2005; 43:225–236. [PubMed: 15864800]
13. Rodrigues LR, Teixeira JA, Schmitt FL, Paulsson M, Lindmark-Mansson H. The Role of Osteopontin in Tumor Progression and Metastasis in Breast Cancer. Cancer Epidemiol Biomarkers Prev. 2007; 16:1087–1097. [PubMed: 17548669]
14. McAllister SS, Gifford AM, Greiner AL, Kelleher SP, Saelzler MP, Ince TA, et al. Systemic endocrine instigation of indolent tumor growth requires osteopontin. Cell. 2008; 133:994–1005. [PubMed: 18555776]
15. Elkabets M, Gifford AM, Scheel C, Nilsson B, Reinhardt F, Bray MA, et al. Human tumors instigate granulin-expressing hematopoietic cells that promote malignancy by activating stromal fibroblasts in mice. J Clin Invest. 2011; 121:784–799. [PubMed: 21266779]
16. Anderberg C, Li H, Fredriksson L, Andrae J, Betsholtz C, Li X, et al. Paracrine Signaling by Platelet-Derived Growth Factor-CC Promotes Tumor Growth by Recruitment of Cancer-Associated Fibroblasts. Cancer Research. 2009; 69:369–378. [PubMed: 19118022]
17. Mi Z, Bhattacharya SD, Kim VM, Guo H, Talbot LJ, Kuo PC. Osteopontin promotes CCL5-mesenchymal stromal cell-mediated breast cancer metastasis. Carcinogenesis. 2011; 32:477–487. [PubMed: 21252118]
18. Denhardt DT, Guo X. Osteopontin: a protein with diverse functions. FASEB J. 1993; 7:1475–1482. [PubMed: 8262332]
19. Kojima Y, Acar A, Eaton EN, Mellody KT, Scheel C, Ben-Porath I, et al. Autocrine TGF-beta and stromal cell-derived factor-1 (SDF-1) signaling drives the evolution of tumor-promoting mammary stromal myofibroblasts. Proc Natl Acad Sci U S A. 2010; 107:20009–20014. [PubMed: 21041659]
20. Kim SJ, Glick A, Sporn MB, Roberts AB. Characterization of the promoter region of the human transforming growth factor-beta 1 gene. J Biol Chem. 1989; 264:402–408. [PubMed: 2909528]
21. Qi W, Gao S, Wang Z. Transcriptional regulation of the TGF-β1 promoter by androgen receptor. Biochem J. 2008; 416:453–462. [PubMed: 18651839]
22. Morris JF, Hromas R, Rauscher FJ 3rd. Characterization of the DNA-binding properties of the myeloid zinc finger protein MZF1: two independent DNA-binding domains recognize two DNA consensus sequences with a common G-rich core. Mol Cell Biol. 1994; 14:1786–1795. [PubMed: 8114711]

23. Hromas R, Morris J, Cornetta K, Berebitsky D, Davidson A, Sha M, et al. Aberrant expression of the myeloid zinc finger gene, MZF-1, is oncogenic. Cancer Res. 1995; 55:3610–3614. [PubMed: 7627970]
24. Tsai S-J, Hwang J-M, Hsieh S-C, Ying T-H, Hsieh Y-H. Overexpression of myeloid zinc finger 1 suppresses matrix metalloproteinase-2 expression and reduces invasiveness of SiHa human cervical cancer cells. Biochemical and Biophysical Research Communications. 2012; 425:462–467. [PubMed: 22846578]
25. Rafn B, Nielsen Christian F, Andersen Sofie H, Szyniarowski P, Corcelle-Termeau E, Valo E, et al. ErbB2-Driven Breast Cancer Cell Invasion Depends on a Complex Signaling Network Activating Myeloid Zinc Finger-1-Dependent Cathepsin B Expression. Molecular Cell. 2012; 45:764–776. [PubMed: 22464443]
26. Hsieh Y-H, Wu T-T, Tsai J-H, Huang C-Y, Hsieh Y-S, Liu J-Y. PKCα expression regulated by Elk-1 and MZF-1 in human HCC cells. Biochemical and Biophysical Research Communications. 2006; 339:217–225. [PubMed: 16297876]
27. Gaboli M, Kotsi PA, Gurrieri C, Cattoretti G, Ronchetti S, Cordon-Cardo C, et al. Mzf1 controls cell proliferation and tumorigenesis. Genes & Development. 2001; 15:1625–1630. [PubMed: 11445537]
28. Mi Z, Guo H, Russell MB, Liu Y, Sullenger BA, Kuo PC. RNA Aptamer Blockade of Osteopontin Inhibits Growth and Metastasis of MDA-MB231 Breast Cancer Cells. Mol Ther. 2009; 17:153–161. [PubMed: 18985031]
29. Mi Z, Guo H, Kuo PC. Identification of osteopontin-dependent signaling pathways in a mouse model of human breast cancer. BMC Res Notes. 2009; 2:119. [PubMed: 19570203]
30. Bhattacharya SD, Mi Z, Kim VM, Guo H, Talbot LJ, Kuo PC. Osteopontin regulates epithelial mesenchymal transition-associated growth of hepatocellular cancer in a mouse xenograft model. Ann Surg. 2012; 255:319–325. [PubMed: 22241292]
31. Korpal M, Yan J, Lu X, Xu S, Lerit DA, Kang Y. Imaging transforming growth factor-[beta] signaling dynamics and therapeutic response in breast cancer bone metastasis. Nat Med. 2009; 15:960–966. [PubMed: 19597504]
32. Pang H, Lu H, Song H, Meng Q, Zhao Y, Liu N, et al. Prognostic values of osteopontin-c, E-cadherin and beta-catenin in breast cancer. Cancer epidemiology. 2013; 37:985–992. [PubMed: 24012693]
33. Patani N, Jouhra F, Jiang W, Mokbel K. Osteopontin expression profiles predict pathological and clinical outcome in breast cancer. Anticancer Res. 2008; 28:4105–4110. [PubMed: 19192668]
34. Xu LN, Xu BN, Cai J, Yang JB, Lin N. Tumor-associated fibroblast-conditioned medium promotes tumor cell proliferation and angiogenesis. Genet Mol Res. 2013; 12:5863–5871. [PubMed: 24301956]
35. Mao Y, Keller E, Garfield D, Shen K, Wang J. Stromal cells in tumor microenvironment and breast cancer. Cancer and Metastasis Reviews. 2012:1–13. [PubMed: 22138778]
36. Huang WH, Chang MC, Tsai KS, Hung MC, Chen HL, Hung SC. Mesenchymal stem cells promote growth and angiogenesis of tumors in mice. Oncogene. 2012
37. Brauer HA, Makowski L, Hoadley KA, Casbas-Hernandez P, Lang LJ, Roman-Perez E, et al. Impact of tumor microenvironment and epithelial phenotypes on metabolism in breast cancer. Clin Cancer Res. 2012
38. Markers for Characterization of Bone Marrow Multipotential Stromal Cells. Stem Cells International. 2012; 2012:12.
39. Quante M, Tu SP, Tomita H, Gonda T, Wang SSW, Takashi S, et al. Bone Marrow-Derived Myofibroblasts Contribute to the Mesenchymal Stem Cell Niche and Promote Tumor Growth. Cancer Cell. 2011; 19:257–272. [PubMed: 21316604]
40. Orimo A, Weinberg RA. Stromal fibroblasts in cancer: a novel tumor-promoting cell type. Cell Cycle. 2006; 5:1597–1601. [PubMed: 16880743]
41. Erez N, Truitt M, Olson P, Hanahan D. Cancer-Associated Fibroblasts Are Activated in Incipient Neoplasia to Orchestrate Tumor-Promoting Inflammation in an NF-[kappa]B-Dependent Manner. Cancer Cell. 2010; 17:135–147. [PubMed: 20138012]

42. Karnoub AE, Dash AB, Vo AP, Sullivan A, Brooks MW, Bell GW, et al. Mesenchymal stem cells within tumour stroma promote breast cancer metastasis. Nature. 2007; 449:557–563. [PubMed: 17914389]
43. Otto WR, Wright NA. Mesenchymal stem cells: from experiment to clinic. Fibrogenesis Tissue Repair. 2011; 4:20. [PubMed: 21902837]
44. Mishra PJ, Banerjee D. Activation and differentiation of mesenchymal stem cells. Methods Mol Biol. 2011; 717:245–253. [PubMed: 21370035]
45. Kidd S, Spaeth E, Watson K, Burks J, Lu H, Klopp A, et al. Origins of the Tumor Microenvironment: Quantitative Assessment of Adipose-Derived and Bone Marrow-Derived Stroma. PLoS One. 2012; 7:e30563. [PubMed: 22363446]
46. Davis C, Price R, Acharya G, Baudino T, Borg T, Berger FG, et al. Hematopoietic Derived Cell Infiltration of the Intestinal Tumor Microenvironment in ApcMin/+ Mice. Microscopy and Microanalysis. 2011; 17:528–539. [PubMed: 21473808]
47. Direkze NC, Hodivala-Dilke K, Jeffery R, Hunt T, Poulsom R, Oukrif D, et al. Bone marrow contribution to tumor-associated myofibroblasts and fibroblasts. Cancer Res. 2004; 64:8492–8495. [PubMed: 15574751]
48. Helluin O, Chan C, Vilaire G, Mousa S, DeGrado WF, Bennett JS. The activation state of alphavbeta 3 regulates platelet and lymphocyte adhesion to intact and thrombin-cleaved osteopontin. JBiolChem. 2000; 275:18337–18343.
49. O'Regan A, Berman JS. Osteopontin: a key cytokine in cell-mediated and granulomatous inflammation. IntJExpPathol. Dec; 2000 81(6):373–90. 2000; 81: 373-390.
50. Tuck AB, O'Malley FP, Singhal H, Harris JF, Tonkin KS, Kerkvliet N, et al. Osteopontin expression in a group of lymph node negative breast cancer patients. IntJ Cancer. 1998; 79:502–508. [PubMed: 9761120]
51. Fedarko NS, Jain A, Karadag A, Van Eman MR, Fisher LW. Elevated serum bone sialoprotein and osteopontin in colon, breast, prostate, and lung cancer. ClinCancer Res. Dec; 2001 7(12):4060–6. 2001; 7: 4060-4066.
52. Tuck AB, Chambers AF. The role of osteopontin in breast cancer: clinical and experimental studies. JMammaryGlandBiolNeoplasia. Oct; 2001 6(4):419–29. 2001; 6: 419-429.
53. Yu K-N, Minai-Tehrani A, Chang S-H, Hwang S-K, Hong S-H, Kim J-E, et al. Aerosol Delivery of Small Hairpin Osteopontin Blocks Pulmonary Metastasis of Breast Cancer in Mice. PLoS One. 2010; 5:e15623. [PubMed: 21203518]
54. Tuck AB, Chambers AF, Allan AL. Osteopontin overexpression in breast cancer: knowledge gained and possible implications for clinical management. JCell Biochem. 2007; 102:859–868. [PubMed: 17721886]
55. Shevde LA, Samant RS, Paik JC, Metge BJ, Chambers AF, Casey G, et al. Osteopontin knockdown suppresses tumorigenicity of human metastatic breast carcinoma, MDA-MB-435. Clin Exp Metastasis. 2006; 23:123–133. [PubMed: 16830223]
56. Ashkar S, Weber GF, Panoutsakopoulou V, Sanchirico ME, Jansson M, Zawaideh S, et al. ETA-1: an early component of type-1 immunity. Science. 2000; 287:860–864. [PubMed: 10657301]
57. Goodison S, Urquidi V, Tarin D. CD44 cell adhesion molecules. MolPathol. 1999; 52:189–196.
58. Wai PY, Kuo PC. The role of Osteopontin in tumor metastasis. JSurgRes. Oct; 2004 121(2):228–41. 2004; 121: 228-241.
59. Brown LF, Papadopoulos-Sergiou A, Berse B, Manseau EJ, Tognazzi K, Perruzzi CA, et al. Osteopontin expression and distribution in human carcinomas. Am J Pathol. 1994; 145:610–623. [PubMed: 8080043]
60. Matsuzaki H, Shima K, Muramatsu T, Ro Y, Hashimoto S, Shibahara T, et al. Osteopontin as biomarker in early invasion by squamous cell carcinoma in tongue. Journal of Oral Pathology & Medicine. 2007; 36:30–34. [PubMed: 17181739]
61. Gao M-Q, Kim BG, Kang S, Choi YP, Park H, Kang KS, et al. Stromal fibroblasts from the interface zone of human breast carcinomas induce an epithelial-mesenchymal transition-like state in breast cancer cells in vitro. J Cell Sci. 2010; 123:3507–3514. [PubMed: 20841377]

62. Udagawa T, Puder M, Wood M, Schaefer BC, D'Amato RJ. Analysis of tumor-associated stromal cells using SCID GFP transgenic mice: contribution of local and bone marrow-derived host cells. FASEB J. 2006; 20:95–102. [PubMed: 16394272]
63. Wang H, Cao F, De A, Cao Y, Contag C, Gambhir SS, et al. Trafficking mesenchymal stem cell engraftment and differentiation in tumor-bearing mice by bioluminescence imaging. Stem Cells. 2009; 27:1548–1558. [PubMed: 19544460]
64. Casey T, Eneman J, Crocker A, White J, Tessitore J, Stanley M, et al. Cancer associated fibroblasts stimulated by transforming growth factor beta1 (TGF-β1) increase invasion rate of tumor cells: a population study. Breast Cancer Research and Treatment. 2008; 110:39–49. [PubMed: 17674196]
65. Quante M, Tu SP, Tomita H, Gonda T, Wang SS, Takashi S, et al. Bone marrow-derived myofibroblasts contribute to the mesenchymal stem cell niche and promote tumor growth. Cancer Cell. 2011; 19:257–272. [PubMed: 21316604]
66. Hawinkels LJ, Paauwe M, Verspaget HW, Wiercinska E, van der Zon JM, van der Ploeg K, et al. Interaction with colon cancer cells hyperactivates TGF-beta signaling in cancer-associated fibroblasts. Oncogene. 2012
67. Su G, Sung KE, Beebe DJ, Friedl A. Functional Screen of Paracrine Signals in Breast Carcinoma Fibroblasts. PLoS One. 2012; 7:e46685. [PubMed: 23056402]
68. Nicholas SB, Liu J, Kim J, Ren Y, Collins AR, Nguyen L, et al. Critical role for osteopontin in diabetic nephropathy. Kidney Int. 2010; 77:588–600. [PubMed: 20130530]
69. Vetrone SA, Montecino-Rodriguez E, Kudryashova E, Kramerova I, Hoffman EP, Liu SD, et al. Osteopontin promotes fibrosis in dystrophic mouse muscle by modulating immune cell subsets and intramuscular TGF-beta. J Clin Invest. 2009; 119:1583–1594. [PubMed: 19451692]
70. Wolak T, Kim H, Ren Y, Kim J, Vaziri ND, Nicholas SB. Osteopontin modulates angiotensin II-induced inflammation, oxidative stress, and fibrosis of the kidney. Kidney Int. 2009; 76:32–43. [PubMed: 19357716]
71. Szalay G, Sauter M, Haberland M, Zuegel U, Steinmeyer A, Kandolf R, et al. Osteopontin: a fibrosis-related marker molecule in cardiac remodeling of enterovirus myocarditis in the susceptible host. Circ Res. 2009; 104:851–859. [PubMed: 19246678]
72. Kohan M, Breuer R, Berkman N. Osteopontin induces airway remodeling and lung fibroblast activation in a murine model of asthma. Am J Respir Cell Mol Biol. 2009; 41:290–296. [PubMed: 19151319]
73. Miyazaki K, Okada Y, Yamanaka O, Kitano A, Ikeda K, Kon S, et al. Corneal wound healing in an osteopontin-deficient mouse. Invest Ophthalmol Vis Sci. 2008; 49:1367–1375. [PubMed: 18385052]
74. Syn WK, Choi SS, Liaskou E, Karaca GF, Agboola KM, Oo YH, et al. Osteopontin is induced by hedgehog pathway activation and promotes fibrosis progression in nonalcoholic steatohepatitis. Hepatology. 2011; 53:106–115. [PubMed: 20967826]
75. Lenga Y, Koh A, Perera AS, McCulloch CA, Sodek J, Zohar R. Osteopontin expression is required for myofibroblast differentiation. Circ Res. 2008; 102:319–327. [PubMed: 18079410]
76. Mudduluru G, Vajkoczy P, Allgayer H. Myeloid Zinc Finger 1 Induces Migration, Invasion, and In vivo Metastasis through Axl Gene Expression in Solid Cancer. Molecular Cancer Research. 2010; 8:159–169. [PubMed: 20145042]
77. Hsieh YH, Wu TT, Huang CY, Hsieh YS, Liu JY. Suppression of tumorigenicity of human hepatocellular carcinoma cells by antisense oligonucleotide MZF-1. Chin J Physiol. 2007; 50:9–15. [PubMed: 17593797]
78. Que-Gewirth NS, Sullenger BA. Gene therapy progress and prospects: RNA aptamers. Gene Ther. 2007; 14:283–291. [PubMed: 17279100]
79. Ireson CR, Kelland LR. Discovery and development of anticancer aptamers. MolCancer Ther. 2006; 5:2957–2962.
80. Wong TY, Liew G, Mitchell P. Clinical update: new treatments for age-related macular degeneration. Lancet. 2007; 370:204–206. [PubMed: 17658379]
81. Mak GW, Lai WL, Zhou Y, Li M, Ng IO, Ching YP. CDK5RAP3 is a novel repressor of p14ARF in hepatocellular carcinoma cells. PLoS One. 2012; 7:e42210. [PubMed: 22860085]

82. Keng PC, Allalunis-Turner J, Siemann DW. Evaluation of cell subpopulations isolated from human tumor xenografts by centrifugal elutriation. Int J Radiat Oncol Biol Phys. 1990; 18:1061–1067. [PubMed: 2347715]

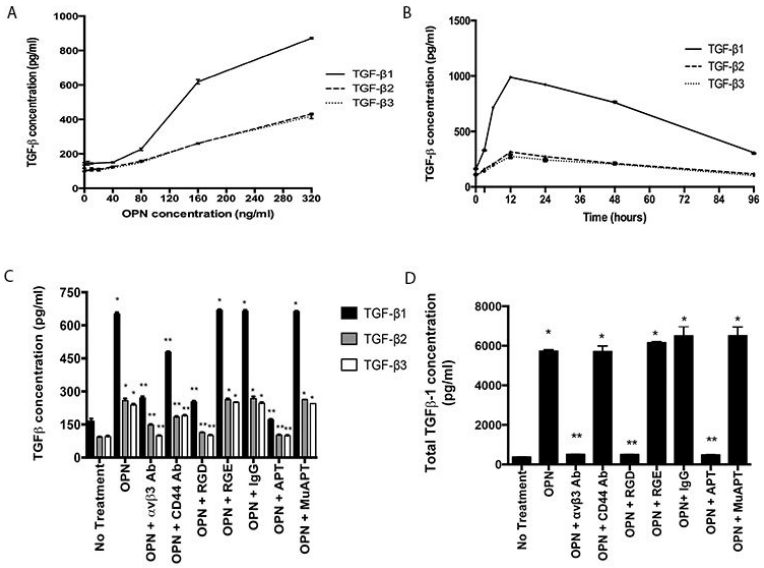

Figure 1.

OPN induces TGF-β1, 2 and 3 protein expression in MSCs in vitro. Data presented as mean ±SEM of three experiments. A. Concentration-dependent expression in MSCs following exposure to OPN for 48 h (ANOVA p=0.0001). B. Time-dependent expression in MSCs following exposure to OPN (180 ng/ml). C. Active TGF-β1, 2 and 3 protein expression in MSCs exposed to OPN (180 ng/ml for 48 h) and one of the following inhibitors: RGD, αvβ3 integrin Ab, CD44 Ab, or APT. Control inhibitors: RGE, IgG, and MuAPT (* p<0.01 vs. No Treatment; ** p<0.01 vs. OPN). D. Total TGF-β1 protein expression in MSCs exposed to OPN (180 ng/ml for 48h) (* p<0.01 vs. No Treatment; ** p<0.01 vs. OPN).

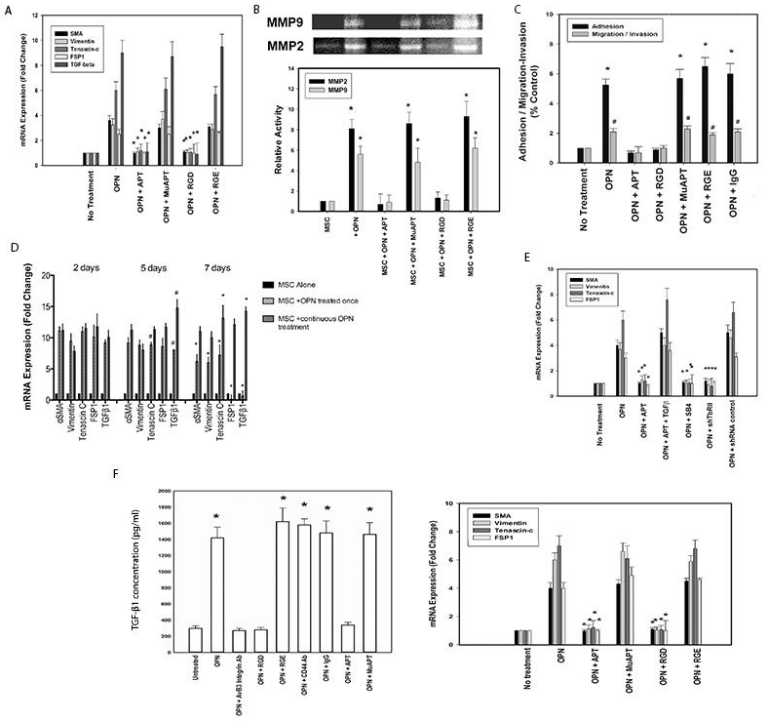

Figure 2.

OPN induces a CAF phenotype in MSCs in vitro. Data presented as mean±SEM of three experiments. A. CAF marker mRNA expression (SMA, tenascin-C, vimentin and FSP-1) in OPN-treated MSCs using qRT-PCR (* $p<0.01$ vs. OPN). B. MMP2 and MMP9 activities are increased by 8- and 5-fold, respectively (* $p<0.01$ vs. MSC, MSC+OPN+APT and MSC +OPN+RGD). C. Adhesion and migration/invasion assays of MSCs (* and # $p<0.01$ vs. No Treatment, OPN+APT and OPN+RGD). D. CAF marker and TGF-β1 mRNA expression in MSCs exposed to OPN either once or daily for one week. (* and # $p<0.01$ vs. Day 2). E. CAF marker mRNA expression after TGF-β1 signaling blockade (SB4 or shTGFβR2) (* $p<0.01$ vs. OPN) or exogenous recombinant TGF-β (400 pg/ml) (* $p<0.01$ vs. OPN+APT). F. TGF-β1 protein and CAF marker mRNA expression in primary human MSCs (TGF-β1: *$p<0.01$ vs. Untreated, OPN+αvβ3 integrin Ab, OPN+RGD. CAF marker mRNA: *$p<0.01$ vs. OPN, OPN+MuAPT and OPN+RGE).

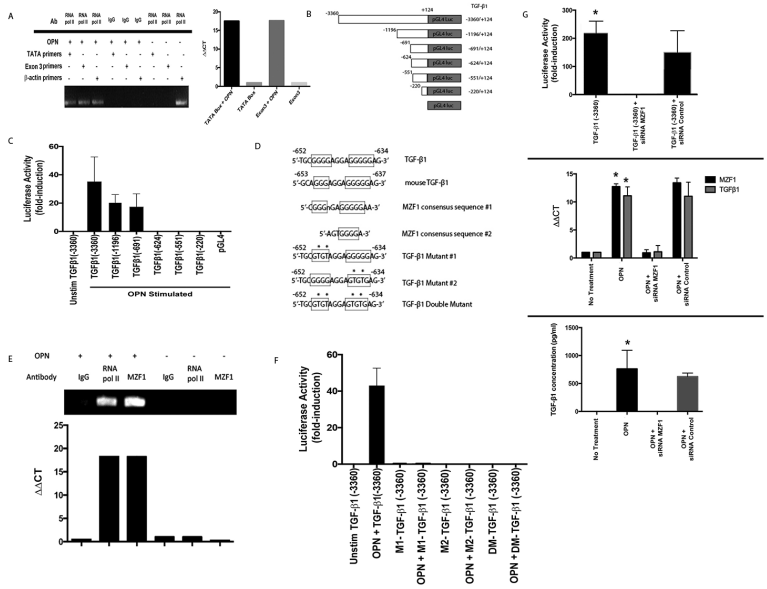

Figure 3.

OPN mediates TGF-β1 transcription. (Data are presented as mean±SEM of at least three experiments. Gels are representative of three experiments.) A. RNA polymerase II binding to TGF-β1 promoter. B. Schematic depiction of TGF-β1 promoter luciferase-reporter constructs. C. Transient transfection analysis of TGF-β1 promoter constructs in MSCs. D. Schematic representation of MZF1 binding sites in human and murine TGF-β1 promoter and associated mutations of putative MZF1 sites. E. ChIP assays for MZF1 and RNA polymerase II binding to the TGF-β1 promoter. F. Transient transfection analysis of mutant and wild-type TGF-β1 promoter constructs in MSCs. G. Effect of siRNA inhibition of MZF1 expression in OPN stimulated MSCs. TGF- β 1 promoter luciferase activity was determined by transient transfection analysis (*p<0.01 vs. TGF-β1 (−3360) + siRNA MZF1). TGF-β1 and MZF1 mRNA expression was measured by RT-PCR (*p<0.01 vs. OPN +siRNA MZF1). TGF-β1 protein in MSC media was analyzed with ELISA (*p<0.01 vs. OPN+siRNA MZF1).

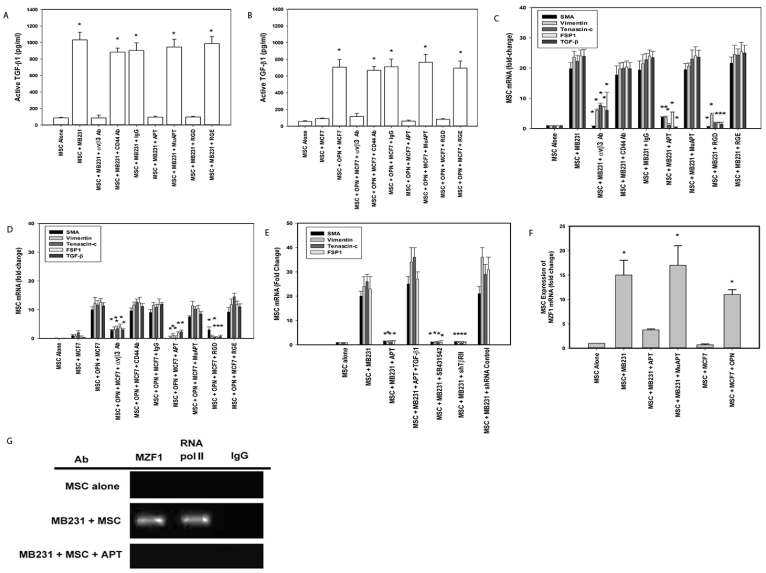

Figure 4.

MB231(OPN+), MCF7 (OPN−) and MSC co-culture studies of TGF-β1 expression. (Data are presented as mean±SEM of at least three experiments. Gels are representative of three experiments.) A. Active TGF-β1 expression in MB231-MSC co-culture media. (*p<0.01 vs. MSC alone, MSC+MB231+αvβ3 integrin Ab, MSC+MB231+APT, and MSC +MB231+RGD). B. Active TGF-β1 expression in MCF7+MSC co-culture media with exogenous OPN (*p<0.01 vs. MSC, MSC+MCF7, MSC+OPN+MCF7+αvβ3 integrin Ab, MSC+OPN+MCF7+APT, and MSC+OPN+MCF7+RGD). C. TGF-β1 and CAF marker mRNA expression by qRT-PCR in MSCs co-cultured with MB231. (* p<0.01 vs. MSC +MB231, MSC+MB231+CD44 Ab, MSC+MB231+IgG, MSC+MB231+MuAPT and MSC +MB231+RGE). D. TGF-β1 and CAF marker mRNA expression by qRT-PCR in MSCs co-cultured with MCF7 and exogenous OPN (*p<0.01 vs. MSC+OPN+MCF7, MSC+OPN +MCF7+CD44 Ab, MSC+OPN+MCF7+IgG, MSC+OPN+MCF7+MuAPT and MSC+OPN +MCF7+RGE). E. CAF marker mRNA expression in MSCs co-cultured with MB231 and inhibitors of TGF- β1 signaling (*p<0.01 vs. MSC+MB231, MSC+MB231+APT+TGF-β1, and MSC+MB231+shRNA Control). F. MZF1 mRNA expression by qRT-PCR in MSCs co-cultured with MB231 (OPN+) or MCF7(OPN) (*p<0.01 vs. MSC, MSC+MB231+APT, and MSC+MCF7). G. ChIP assay for MZF1 and RNA polymerase II binding to the TGF-β1 promoter region, −697 to −600, in MSCs co-cultured with MB231.

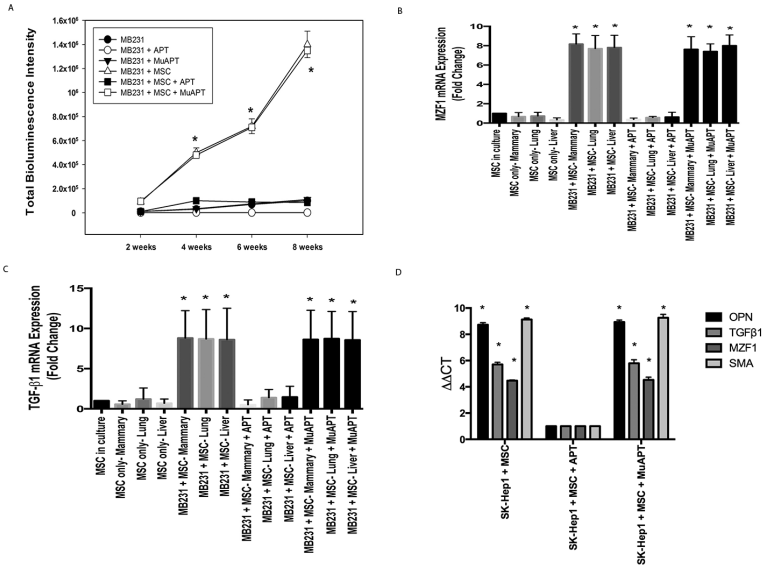

Figure 5.

MB231 or SK-Hep1 in vivo co-implantation models with MSCs in NOD-scid mice. Data derived from four animals in each group. A. Bioluminescence intensity in MB231 mouse model (* $p<0.01$ for MB231+MSC or MB231+MSC+MuAPT vs. MB231, MB231+APT, MB231+MuAPT and MB231+MSC+APT). B. MZF1 mRNA expression by qRT-PCR in MSCs isolated from MB231±MSC mice. (*$p<0.01$ vs. MSC only and MB231+MSC+APT among the various locations). C. TGF-β1 mRNA expression by qRT-PCR in MSCs isolated from MB231±MSC mice. (*$p<0.01$ vs. MSC only and MB231+MSC+APT among the various locations). D. OPN, TGF-β1, MZF1, SMA mRNA expression by qRT-PCR in MSCs isolated from SK-Hep1+MSC mice. (*$p<0.01$ vs. SK-Hep1+MSC+APT).

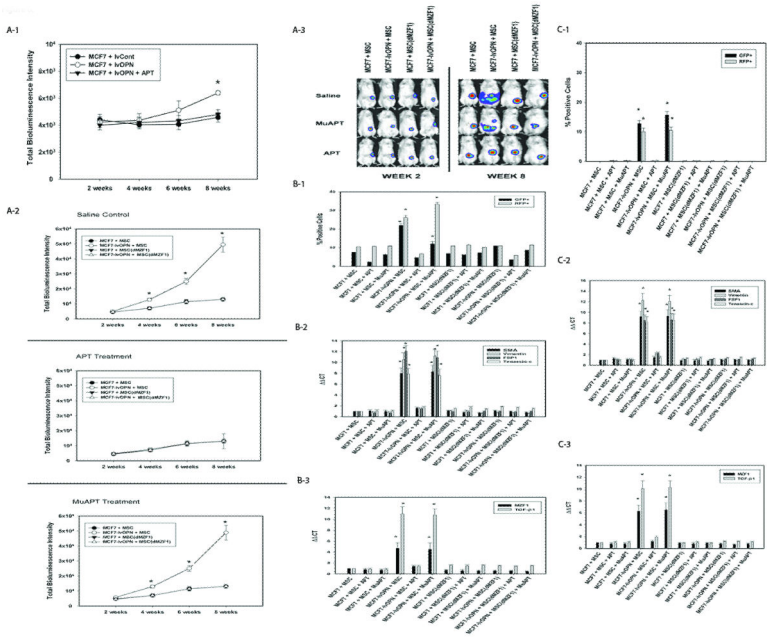

Figure 6.

MCF7 in vivo co-implantation models with MSCs in NOD-scid mice. Data derived from four animals in each group. A-1. Bioluminescence intensity in MCF7±lvOPN mouse model (*p<0.01 vs. MCF7-lvCont and MCF-lvOPN+APT). A-2. Bioluminescence intensity in MCF7±lvOPN± MSC(dMZF1) mouse model (*p<0.01 vs. MCF7+MSC, MCF7+MSC(dMZF1) and MCF7-lvOPN+MSC(dMZF1) treated with saline control, APT or MuAPT. A-3. Representative photos of bioluminescence in MCF7 mouse models at Week 2 and Week 8. B-1. FACS analysis of MCF7 cells (RFP+) and MSCs (GFP+) isolated from primary tumor. (*p<0.01 vs. MCF7+MSC, MCF7+MSC+APT, MCF7-lvOPN+MSC +APT, MCF7+MSC(dMZF1) and MCF7-lvOPN+MSC(dMZF1)). B-2. CAF marker mRNA expression by qRT-PCR in MSCs. (*p<0.01 vs. MCF7+MSC, MCF7+MSC+APT, MCF7-lvOPN+MSC+APT, MCF7+MSC(dMZF1) and MCF7-lvOPN+MSC(dMZF1)). B-3. MZF1 and TGF-β1 mRNA expression by qRT-PCR in MSCs. (*p<0.01 vs. MCF7+MSC, MCF7+MSC+APT, MCF7-lvOPN+MSC+APT, MCF7+MSC(dMZF1) and MCF7-lvOPN +MSC(dMZF1)). C-1. FACS analysis of MCF7 cells (RFP+) and MSCs (GFP+) isolated from liver. (*p<0.01 vs. MCF7+MSC, MCF7+MSC+APT, MCF7-lvOPN+MSC+APT, MCF7+MSC(dMZF1) and MCF7-lvOPN+MSC(dMZF1)). C-2. CAF marker mRNA expression by qRT-PCR in MSCs. (*p<0.01 vs. MCF7+MSC, MCF7+MSC+APT, MCF7-lvOPN+MSC+APT, MCF7+MSC(dMZF1) and MCF7-lvOPN+MSC(dMZF1)). C-3. MZF1 and TGF-β1 mRNA expression by qRT-PCR in MSCs. (*p<0.01 vs. MCF7+MSC, MCF7+MSC+APT, MCF7-lvOPN+MSC+APT, MCF7+MSC(dMZF1) and MCF7-lvOPN +MSC(dMZF1)).

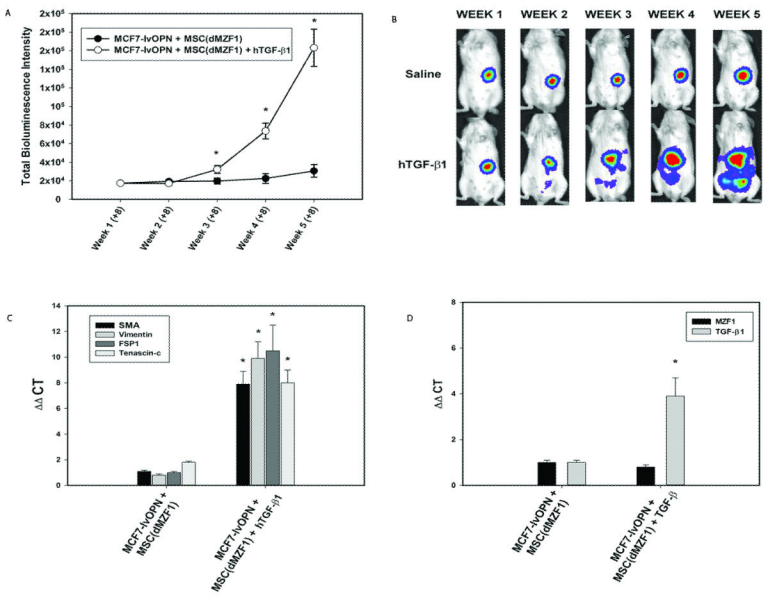

Figure 7.

Gain of function study with administration of exogenous TGF-β1 to a subgroup of MCF7-lvOPN+MSC(dMZF1) beginning 8 weeks after co-implantation. Data are presented as mean ±SEM of three animals in each group. A. Bioluminescence intensity in MCF7-lvOPN +MSC(dMZF1) mouse model (*p<0.01 vs. MCF7-lvOPN+MSC(dMZF1)) B. Representative images of luciferase activity in mice at Weeks 1 through 5. (*p<0.01 vs. MCF7-lvOPN+MSC(dMZF1)). C. CAF mRNA expression by qRT-PCR in MSCs isolated from primary tumors. (*p<0.01 vs. MCF7-lvOPN+MSC(dMZF1)). D. MZF1 and TGF-β1 mRNA expression by qRT-PCR in MSCs isolated from primary tumors. (*p<0.01 vs. MCF7-lvOPN+MSC(dMZF1).

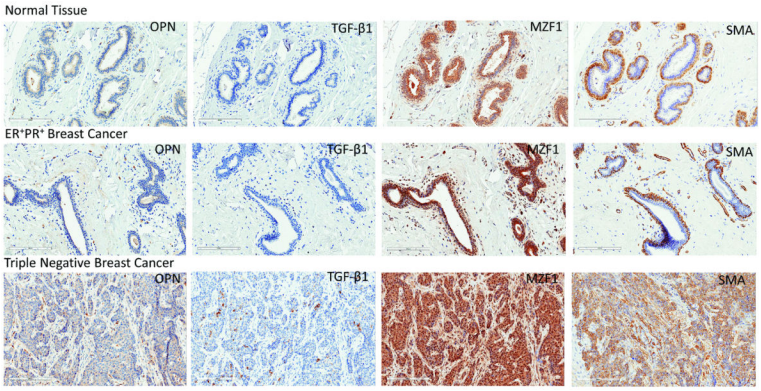

Figure 8.

Immunohistochemical staining of human breast cancer tissue samples Representative images of IHC tissue samples stained with OPN, TGF-β1, MZF1 and SMA. Normal breast tissue, top row, (n=2), ER+PR+ human breast cancer tissue, middle row, (n=2), and triple-negative human breast cancer tissue, bottom row, (n=4). All images taken at 200×. Staining quantity and intensity of all four proteins is increased in both the tumor cells and the stromal elements of the TNBC compared to normal breast tissue and ER+PR+ breast cancer tissue.